Fatty Acid Metabolic Imaging with Iodine-123-BMIPP for the Diagnosis of Coronary Artery Disease

Satomi Fujiwara, Yasuchika Takeishi, Hiroyuki Atsumi, Kazuei Takahashi and Hitonobu Tomoike
First Department of Internal Medicine, Division of Radiology, Yamagata University School of Medicine, Yamagata, Japan

Iodine-123-BMIPP kinetics under high glucose levels were examined. The feasibility of ^{123}I-BMIPP imaging after oral glucose loading for the detection of impaired fatty acid metabolism was tested in patients with coronary artery disease. **Methods**: Fatty acid metabolic imaging with ^{123}I-BMIPP was performed on 29 patients in the fasting state and repeated after oral glucose loading. Myocardial SPECT images were obtained 20 min and 4 hr after the injection of ^{123}I-BMIPP. Myocardial uptake of ^{123}I-BMIPP was calculated by a Ishii-MacIntyre method and the clearance of ^{123}I-BMIPP from the myocardium was determined as (early counts-delayed counts) × 100/early counts. Regional accumulation of ^{123}I-BMIPP was scored semiquantitatively from 0 (normal) to 4 (no activity), and the sum of regional scores in each patient was defined as a total defect score (TDS). **Results**: Total myocardial uptake of ^{123}I-BMIPP was 1.7% ± 0.4% in the fasting state and 1.6% ± 0.3% after oral glucose loading ($p < 0.05$). Iodine-123-BMIPP clearance from the myocardium was faster after glucose loading than in the fasting state (27% ± 8% versus 11% ± 6%, $p < 0.01$). After glucose loading, ^{123}I-BMIPP clearance was faster in the ischemic myocardium (defined as areas perfused by stenosed coronary artery exceeding 90%) than in the nonischemic myocardium (33% ± 8% versus 25% ± 9%, $p < 0.05$). TDS in the ischemic myocardium increased from 1.8 ± 0.4 in the fasting state to 2.1 ± 0.4 after glucose loading ($p < 0.01$). The sensitivity for detecting coronary stenosis exceeding 90% increased from 55% (11/20) in the fasting state to 75% (15/20) after glucose loading without a loss of specificity (78%, 7/9). **Conclusion**: Oral glucose loading enhanced the detection of areas with impaired fatty acid metabolism due to coronary artery narrowing. Iodine-123-BMIPP imaging with oral glucose loading may be a new approach for the noninvasive diagnosis of coronary artery disease.

Key Words: iodine-123-BMIPP; myocardial ischemia; myocardial metabolism

J Nucl Med 1997; 38:175–180

The heart uses many kinds of substrates for its energy metabolism including free fatty acids, glucose, lactate, pyruvate and amino acids (*1*). Plasma substrate concentrations are not constant, depending on the dietary state and physical activity, and affect the pattern of myocardial substrate utilization. In the fasting state, fatty acids account for more than 70% of myocardial energy requirements at rest under normal aerobic conditions (*1*). After a carbohydrate meal, glucose and insulin levels in the plasma increase with a concomitant decrease in plasma fatty acid levels, and the heart uses glucose mainly as an energy source. Carbon-11-palmitate has been used for the evaluation of fatty acid metabolism with PET (*2,3*). Schelbert et al. (*3*) reported that extraction of ^{11}C-palmitate is decreased and its half-time prolonged after glucose and insulin infusion. For practical purposes, single-photon emitting radionuclides that can assess myocardial metabolism have long been desired (*4–8*). Recently, ^{123}I beta-methyl-iodophenyl-pentadecanoic acid (^{123}I-BMIPP) has been developed and used as a tracer for myocardial fatty acid metabolism (*9,10*). Myocardial accumulation of ^{123}I-BMIPP is decreased in comparison with flow tracer in patients with coronary artery disease (*11–18*). Decreased myocardial uptake of ^{123}I-BMIPP is frequently observed in the presence of normal myocardial distribution of perfusion tracer, and thus ^{123}I-BMIPP is more sensitive for detecting myocardial ischemia associated with coronary artery stenosis than perfusion imaging (*17,18*). Tamaki et al. (*19*) reported that myocardial areas, in which the uptake of ^{123}I-BMIPP was more decreased than that of perfusion tracer, showed increased [^{18}F]FDG uptake. This finding indicates that suppressed fatty acid metabolism is associated with enhanced glucose utilization and thus represent myocardial ischemia. Although, ^{123}I-BMIPP has been increasingly used in patients with various types of heart diseases, the effects of substrate concentrations on ^{123}I-BMIPP kinetics in the myocardium have not been rigorously examined in in vivo studies (*20*).

The present study was designed to clarify the ^{123}I-BMIPP kinetics under high glucose and insulin levels and to test the feasibility of ^{123}I-BMIPP imaging with oral glucose loading for improving the noninvasive assessment of coronary artery disease. Myocardial uptake and clearance of ^{123}I-BMIPP after oral glucose loading were compared with those in the fasting state.

MATERIALS AND METHODS

Subjects and Study Protocol

Twenty-nine patients (22 men, 7 woman; mean age 63 yr) who were scheduled for coronary arteriography at the Yamagata University Hospital were examined. (Table 1). Twenty-two patients had no previous myocardial infarction, whereas seven patients fulfilled both historical and electrocardiographic criteria of prior infarction. Fatty acid metabolic imaging with ^{123}I-BMIPP was performed at rest in the fasting condition. Iodine-123-BMIPP imaging was repeated after glucose loading 3 days later. Coronary arteriography was performed in all patients within 1 wk after the radionuclide studies. Twenty patients showed the presence of coronary stenosis to exceed 90%; this was absent in the remaining nine patients. Ischemic myocardium was defined as an area perfused by a stenotic coronary artery of more than 90%. The study protocol was approved by the Committee of Human Research of Yamagata University Hospital. Written informed consent was obtained from all patients.

Myocardial Imaging With Iodine-123-BMIPP

Data Acquisition and Processing. An 18-gauge teflon catheter was placed in an anterior-cubital vein, the patients faced a rotating gamma camera equipped with a parallel-hole, high-resolution collimator in the resting supine position. After an overnight fast or 75 g oral glucose, blood samples were obtained from the catheter and the levels of blood sugar, triglyceride, total cholesterol, free

Received Feb. 12, 1996; revision accepted Jun. 15, 1996.
For correspondence or reprints contact: Satomi Fujiwara, MD, First Department of Internal Medicine, Yamagata University School of Medicine, 2-2-2 Iida-Nishi, Yamagata, 990-23 Japan.

TABLE 1
Patients Characteristics and Changes in Myocardial Uptake, Washout and Total Defect Score after Glucose Loading

Patient no.	Sex	Age (yr)	Coronary stenosis (≥90%)			Uptake		Washout		Anterior		Septal		Apical		Inferior		Lateral		TDS	
						Fast	Glu	Fast	Glu	Fast	Glu	Fast	Glu	Fast	Glu	Fast	Glu	Fast	Glu	Fast	Glu
1	M	64				2.3	2.0	16	32	0	0	0	0	0	0	0	0	0	0	0	0
2	M	66				1.1	1.0	18	23	0	0	0	0	0	0	1	1	0	0	1	1
3	M	44	LAD			1.6	1.9	14	38	0	0	0	0	0	0	0	0	0	0	0	0
4	F	51				1.7	1.4	5	31	0	0	0	0	0	0	1	1	0	0	1	1
5	M	70				1.0	1.4	1	34	0	0	0	0	0	0	0	0	0	0	0	0
6	M	73	LAD			1.7	1.5	12	27	0	0	0	0	0	1	0	0	0	0	0	1
7	M	71		LCX	RCA	1.6	1.6	13	19	0	0	0	0	4	4	8	8	0	1	12	13
8	M	76				2.4	1.9	15	22	0	0	0	0	0	0	0	0	0	0	0	0
9	M	62			RCA	1.6	1.6	7	35	0	0	0	0	0	0	0	0	0	0	0	0
10	M	61	LAD			1.3	1.4	18	20	7	7	5	5	6	6	3	3	0	0	21	21
11	F	75	LAD			1.7	1.7	3	11	0	0	0	0	0	0	0	0	0	0	0	0
12	F	62		LCX		2.3	2.1	6	8	0	0	0	0	0	0	0	0	0	0	0	0
13	F	67	LAD		RCA	1.6	1.3	10	38	0	0	0	1	1	2	1	2	0	0	2	5
14	M	67				1.8	1.5	17	28	0	0	0	0	0	0	0	0	0	0	0	0
15	M	36				1.5	1.4	13	22	0	0	0	0	0	0	0	0	0	0	0	0
16	F	68			RCA	1.5	1.6	2	30	0	0	0	0	0	0	0	1	0	0	0	1
17	M	70	LAD			1.6	1.6	6	32	0	0	0	0	0	1	0	2	0	0	0	3
18	M	66				1.5	1.5	25	32	0	0	0	0	0	0	0	0	0	0	0	0
19	M	66			RCA	1.4	1.2	4	31	0	0	0	0	4	4	8	8	0	0	12	12
20	M	51			RCA	1.4	1.3	14	17	0	0	0	1	1	1	4	5	0	0	5	7
21	F	82	LAD	LCX	RCA	1.5	1.2	5	30	0	0	0	3	2	3	8	7	0	0	10	13
22	M	63				2.0	1.8	10	22	0	0	0	0	0	0	0	0	0	0	0	0
23	M	49			RCA	2.8	1.7	16	30	0	0	0	0	0	0	6	6	0	0	6	6
24	F	57	LAD			1.6	1.8	4	26	1	2	0	0	3	4	0	0	0	0	4	6
25	M	68	LAD		RCA	2.1	1.8	12	28	0	0	2	2	5	5	8	8	2	2	17	17
26	M	59	LAD		RCA	2.2	2.0	15	33	2	3	0	0	2	2	8	8	0	0	12	13
27	M	62			RCA	1.4	1.3	8	11	0	0	0	0	0	0	0	1	0	0	0	1
28	F	70	LAD			1.6	1.7	7	21	0	0	0	0	0	0	0	0	0	0	0	0
29	M	48		LCX	RCA	2.6	2.4	11	14	0	0	0	0	0	0	3	4	4	4	7	8

LAD = left anterior descending artery; LCX = left circumflex artery; RCA = right coronary artery; fast = fasting condition; glu = glucose loading; TDS = total defect score.

fatty acid and insulin were measured. Then, a dose of 148 MBq ^{123}I-BMIPP was injected intravenously and flushed rapidly with 20 ml saline. Serial dynamic imaging from the standard anterior projection was started at a rate of 1 frame/sec over the whole thorax and continued for 60 sec (*21–23*). A region of interest (ROI) was set over the whole thorax, and a time-activity curve (TAC) was derived. A total injected dose (T, counts/sec) was obtained from the peak counts of the TAC (Fig. 1).

Myocardial SPECT imaging was carried out 20 min and 4 hr after the ^{123}I-BMIPP administration as previously described (*17,18,24*). All images were obtained on a rotating gamma camera equipped with a parallel-hole, high-resolution collimator. Seventy-two images were obtained over a 360° arc. Energy discrimination was provided by a 15% window centered at 159 KeV. Each image was accumulated for 50 sec. Data were stored on a 64 × 64 matrix. Data processing was performed on a nuclear medicine computer system and a series of contiguous transaxial images of 6 mm thickness were reconstructed by means of a filtered back-projection algorithm without attenuation correction. These transaxial images were then reoriented in the short-axis, vertical long-axis and horizontal long-axis of the left ventricle.

Image Interpretation. The myocardial distribution of ^{123}I-BMIPP was analyzed in three standard orthogonal tomographic imaging planes: (a) anterior, septal, inferior and lateral regions in the short-axis view; (b) anterior, apical and inferior regions in the vertical long-axis view; (c) and septal, apical and lateral regions in the horizontal long-axis view. The left ventricle was divided into 10 segments by splitting the anterior, septal, inferior and lateral wall into a basal and apical segment, including two extra segments for the apex. The anterior, septal and apical walls were corresponded to the territory of the left anterior descending artery, the inferior wall to the territory of the right coronary artery and the lateral wall to the territory of the left circumflex artery. The image was interpreted by two independent observers who were unaware of the clinical history and angiographic findings of the patients. A

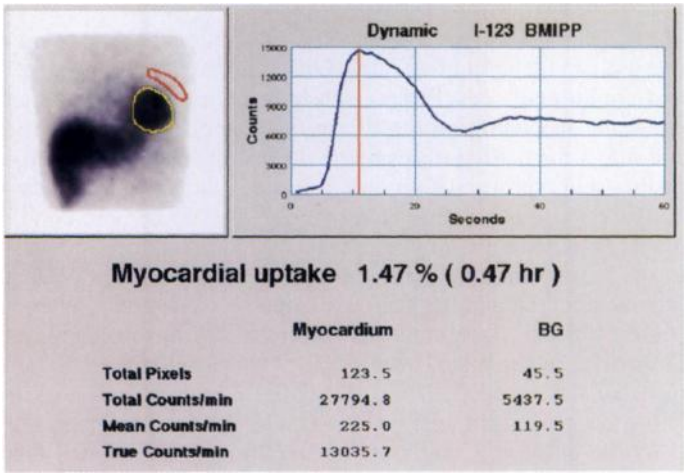

FIGURE 1. Total injected dose of ^{123}I-BMIPP (counts/sec) was estimated from the peak counts of the time-activity curve over the whole thorax (right panel). ROIs were defined in the entire left ventricle and the lung as a background (left panel).

five-point scoring system was used to evaluate regional myocardial tracer uptake as described previously (*17*): 0 = normal, 1 = slightly reduced, 2 = moderately reduced, 3 = severely reduced and 4 = no activity. The sum of scores for 10 segments was defined as a total defect score (TDS) in each patient. The grading was settled by consensus between the two observers. When they disagreed on the results, a third observer reviewed the images and a decision was made.

Quantification of Myocardial Images. Myocardial uptake of ^{123}I-BMIPP was calculated from the anterior projection image by an Ishii-MacIntyre method (*21–23*). The three projections (−5, 0 and 5°) that corresponded to the anterior position of the unprocessed projection images acquired as part of the early SPECT images were added, and ROIs were manually drawn over the entire left ventricle and lung as a background (Fig. 1). The number of pixels within the myocardial ROI (A_1, pixels) and background ROI (A_2, pixels), mean counts per pixel over the myocardial ROI (M, counts per pixel) and background ROI (B, counts per pixel) were measured. Because three projections of 50-sec image were added for analysis, acquisition time was 150 sec. Myocardial uptake of ^{123}I-BMIPP was calculated as follows:

$$\text{uptake (\%)} = (M - B \times A_1/A_2)/T \times 150. \quad \text{Eq. 1}$$

M = counts in myocardial ROI; B = counts in background ROI; A_1 = number of pixels in myocardial ROI; A_2 = number of pixels in background ROI; and T = a total injected dose per second.

Images were analyzed twice by the same observer at least 2 wk apart to determine intraobserver variability in 10 patients. Myocardial uptake was also independently calculated by the second observer to obtain interobserver variability. The calculation of myocardial ^{123}I-BMIPP uptake was highly reproducible in repeated measurements by the same observer on separate occasions ($r = 0.98$, $p < 0.01$) and between the two independent observers ($r = 0.96$, $p < 0.01$).

The clearance of ^{123}I-BMIPP from the myocardium was calculated from the absolute counts in early (Ce) and delayed (Cd) images with a correction for decay as follows:

$$\text{clearance (\%)} = (Ce - Cd \times Cf) \times 100/Ce. \quad \text{Eq. 2}$$

$$Cf = 1/(1/2)x,\ x = (Td - Te)/13.2. \quad \text{Eq. 3}$$

$$\text{(Td (hr): time for delayed image, Te (hr): time for early image).} \quad \text{Eq. 4}$$

Coronary Arteriography

Selective coronary arteriography was performed in multiple projections using standard Judkin's technique within 1 wk after the radionuclide studies. After visual inspection of the coronary angiograms in all views, the frame of optimal clarity was selected, showing lesion at maximal narrowing and arterial silhouette in sharpest focus. The images were analyzed by an experienced cardiologist blinded to the clinical and scintigraphic data. The severity of coronary stenosis was measured with a caliper and expressed as the percentage of luminal diameter reduction.

Statistical Analysis

Continuous variables were compared by Student's t-test. The differences in proportion (categorical variables) were examined by chi-square testing. A p value < 0.05 was considered significant.

RESULTS

Case Presentation

Myocardial tomographic images with ^{123}I-BMIPP in a patient with unstable angina are shown in Figure 2 (Patient 24, Table 1). Coronary stenosis of 99% was evident in the left anterior descending artery. Iodine-123-BMIPP accumulation was reduced in the anterior and apical regions of the left ventricle in the fasting images. As shown in Figure 2, decreased uptakes of ^{123}I-BMIPP in these regions were more extensive after glucose loading.

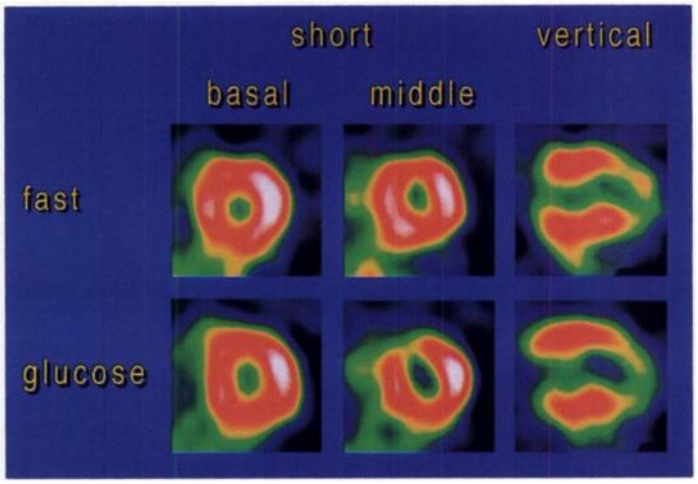

FIGURE 2. Myocardial ^{123}I-BMIPP SPECT images of a patient with unstable angina who had a 99% stenosis in the left anterior descending artery. Upper panels are early images in the fasting state, and lower panels are those after glucose loading. Decreased uptake of ^{123}I-BMIPP in the anterior and apical segments observed on the fasting images became more extensive after glucose loading.

Figure 3 shows myocardial ^{123}I-BMIPP images of a patient with stable effort angina (Patient 16, Table 1). Although, this patient had a 90% coronary stenosis in the right coronary artery, myocardial uptake of ^{123}I-BMIPP in the fasting images was homogeneous. After glucose loading, ^{123}I-BMIPP images clearly showed that decreased fatty acid metabolism was present in the inferior wall of the left ventricular myocardium.

Comparison of Regional Uptakes Between Iodine-123-BMIPP and Technetium-99m-Sestamibi

Myocardial distribution of ^{99m}Tc-sestamibi and ^{123}I-BMIPP was compared on a segment-by-segment basis. Ischemic myocardium was defined as the areas perfused by a stenotic coronary artery exceeding 90%. As shown in Figure 4, of 99 segments with ischemic myocardium, 76 (77%) and 72 (73%)

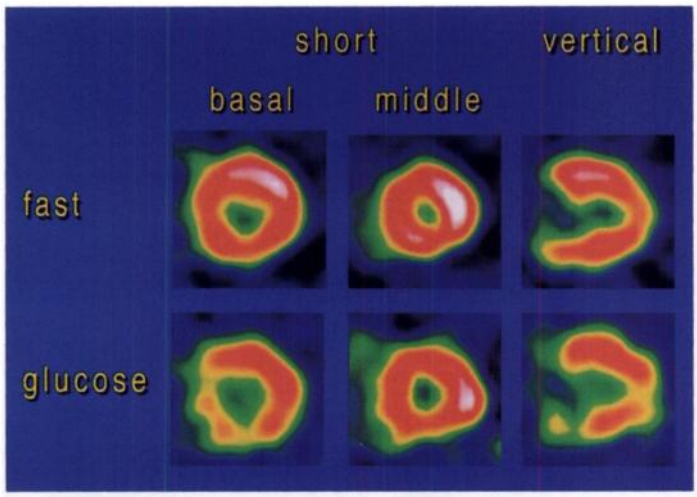

FIGURE 3. Myocardial ^{123}I-BMIPP images of a patient with effort angina. This patient had a coronary stenosis of 90% in the right coronary artery. Upper panels are early images in the fasting state and lower panels are those after glucose loading. Myocardial distribution of ^{123}I-BMIPP was homogeneous in the fasting images. Decreased ^{123}I-BMIPP uptake was seen in the inferior wall of the left ventricle after glucose loading.

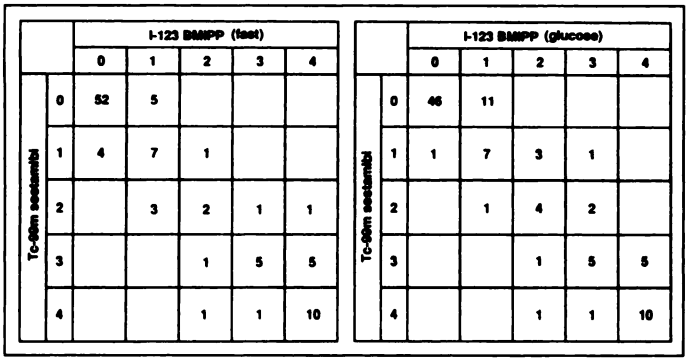

FIGURE 4. Segment-by-segment comparison between myocardial ^{123}I-BMIPP and ^{99m}Tc-sestamibi uptake.

segments showed concordant findings in the fasting state and after glucose loading, respectively. In contrast, 13 (13%) segments with decreased accumulation of ^{123}I-BMIPP in comparison with ^{99m}Tc-sestamibi uptake were observed in the fasting state. After glucose loading, discordant (decreased) ^{123}I-BMIPP accumulation was increased to 22 (22%) segments. Of 191 segments with nonischemic myocardium, regional uptake of ^{99m}Tc-sestamibi were concordant with that of ^{123}I-BMIPP in 182 segments (95%) and 178 segments (93%) in the fasting state and after glucose loading, respectively.

Changes in Total Myocardial Uptake and Clearance of Iodine-123-BMIPP after Glucose Loading

After glucose loading, the serum concentrations of blood sugar (103 ± 23 versus 184 ± 40 mg/dl (mean ± s.d.), $p < 0.01$), triglyceride (124 ± 61 versus 142 ± 76 mg/dl, $p < 0.05$), cholesterol (203 ± 32 versus 212 ± 37 mg/dl, $p < 0.01$), insulin (11.2 ± 3.9 versus 65.8 ± 57.2 μU/ml, $p < 0.01$) increased, and the level of free fatty acid decreased (0.55 ± 0.31 versus 0.17 ± 0.06 mEq/liter, $p < 0.01$).

Total myocardial uptake of ^{123}I-BMIPP was 1.7% ± 0.4% (mean ± s.d.) and the clearance of ^{123}I-BMIPP from the myocardium was 11% ± 6% in the fasting state (Fig. 5). After glucose loading, myocardial uptake of ^{123}I-BMIPP slightly decreased to 1.6% ± 0.3% ($p < 0.05$), while the clearance increased to 27% ± 8% ($p < 0.01$). Iodine-123-BMIPP clearance was examined in the ischemic and nonischemic myocardium (Fig. 6). After oral glucose loading, clearance of ^{123}I-BMIPP was markedly increased in both ischemic and nonischemic myocardium (ischemic area: 9% ± 5% to 33% ± 8%, $p < 0.01$, nonischemic area: 6% ± 8% to 25% ± 9%, $p < 0.01$). Iodine-123-BMIPP clearance after glucose loading was faster in the ischemic area than in the nonischemic area (33% ± 8% versus 25% ± 9%, $p < 0.05$).

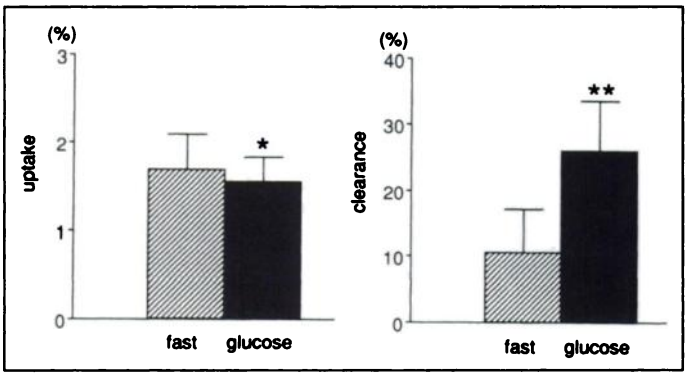

FIGURE 5. Changes in myocardial uptake and clearance of ^{123}I-BMIPP between the fasting state and after glucose loading. Data were reported as mean ± s.d. * $p < 0.05$, ** $p < 0.01$ versus fasting state.

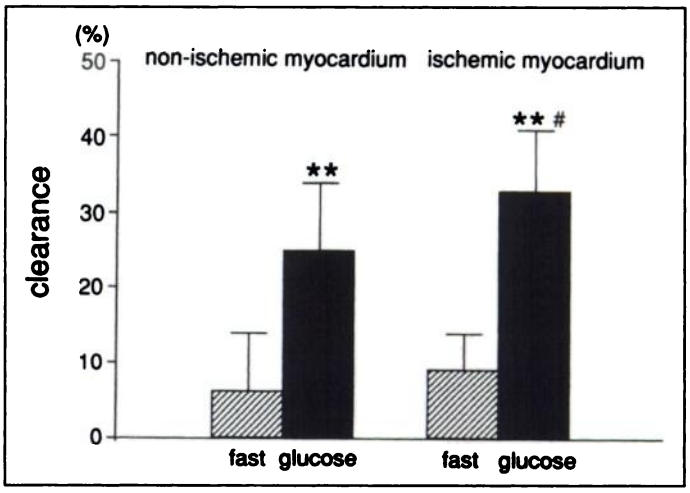

FIGURE 6. Changes in ^{123}I-BMIPP clearance in ischemic and nonischemic myocardium after glucose loading. Data were reported as mean ± s.d. ** $p < 0.01$ versus fasting state; # $p < 0.05$ versus nonischemic myocardium after glucose loading.

Changes in Regional Iodine-123-BMIPP Accumulation after Glucose Loading

Regional distribution of ^{123}I-BMIPP on the early images was compared between in the fasting state and after glucose loading (Table 1). TDS was 3.7 ± 1.2 (mean ± s.e.) in the fasting state and 4.3 ± 1.2 after glucose loading ($p < 0.01$). Of 20 patients with coronary stenosis of more than 90%, 11 patients showed an increase in TDS after glucose loading. In the ischemic myocardium, sum of defect scores increased from 1.8 ± 0.4 to 2.1 ± 0.4 ($p < 0.01$) after glucose loading (Fig. 7). In the nonischemic myocardium, sum of defect scores unchanged after glucose loading (0.2 ± 0.1 versus 0.2 ± 0.1). There were seven patients with prior myocardial infarction, which was anterior in one patient (Patient 10, see Table 1), inferior in five patients (Patients 7, 19, 21, 25 and 26), and lateral in one patient (Patient 29). In segments of infarcted myocardium, a defect score unchanged after glucose loading in all seven patients.

The sensitivity of detecting the patients with coronary stenosis of more than 90% was 55% (11/20) in the fasting state and 75% (15/20) after glucose loading. The specificity was same between in the fasting state and after glucose loading, 78% (7/9).

DISCUSSION

After glucose loading, total myocardial uptake of ^{123}I-BMIPP was reduced slightly, and the clearance was markedly increased. Iodine-123-BMIPP clearance after glucose loading

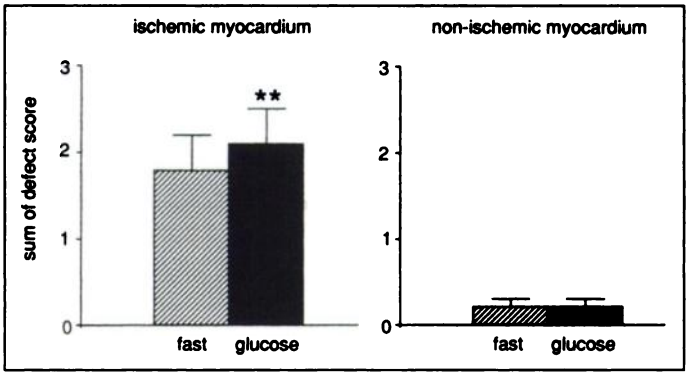

FIGURE 7. Changes in sum of defect scores on the early images after glucose loading. Data were presented as mean ± s.e. ** $p < 0.01$ versus fasting state.

was faster in the ischemic myocardium than in the nonischemic myocardium. The defect scores in the ischemic myocardium were larger after glucose loading than in the fasting state.

A noninvasive evaluation of myocardial metabolism and perfusion has long been desired. Assessment of cardiac energy metabolism by ^{123}I-BMIPP permits characterization of the metabolic status of various cardiac diseases (*9–19,24*). Iodine-123-BMIPP has the following favorable biologic properties for myocardial emission computed tomographic imaging (*9,10*): (a) high uptake and prolonged retention in the myocardium, (b) relatively higher heart-to-background count ratio and (c) rapid blood clearance. Although ^{123}I-BMIPP may not be an ideal tracer for myocardial fatty acid metabolism, myocardial accumulation of ^{123}I-BMIPP is associated with triglyceride synthesis, which in part reflects fatty acid utilization.

In ischemic myocardium, oxidative fatty acid metabolism is decreased as a result of the decrease in oxygen delivery, and exogenous glucose uptake and glycolytic flux are increased (*25*). PET with [^{18}F]FDG can be used for evaluating myocardial glucose utilization (*25–28*). In the fasting condition, only ischemic myocardium shows FDG uptake, whereas its utilization is suppressed both in the normal and infarcted myocardium. After glucose loading, fatty acid utilization is suppressed both in normal and ischemic myocardium, and glucose is used mainly as an energy source (*1,3*). After glucose and insulin infusion, plasma glucose and insulin levels increase with a concomitant fall in the levels of plasma free fatty acid, and oxygen equivalents of free fatty acid (percent of myocardial O_2 consumption) are decreased (*3*). Carbon-11-palmitate reflected these changes in myocardial substrate utilization as a decrease of extraction of ^{11}C-palmitate and a prolongation of its half-time. In areas with ischemic myocardium, ^{123}I-BMIPP uptake is reduced. In the present study, of the 99 segments with ischemic myocardium perfused by a stenotic coronary artery exceeding 90%, 13 (13%) and 22 segments (22%) showed less ^{123}I-BMIPP uptake than ^{99m}Tc-sestamibi uptake in the fasting state and after glucose loading, respectively. As we reported previously, reduced uptake of ^{123}I-BMIPP was frequently observed in the presence of normal ^{99m}Tc-sestamibi distribution and ^{123}I-BMIPP was more sensitive for detecting the myocardial ischemia due to coronary artery stenosis than perfusion imaging with ^{99m}Tc-sestamibi in patients with unstable angina and stable effort angina (*17,18*). Many reports have shown that myocardial accumulation of ^{123}I-BMIPP is decreased in comparison with flow tracer in acute and subacute myocardial infarction, unstable and stable angina (*11–18*). This "mismatching" phenomenon is frequently observed after coronary thrombolysis in patients with an acute or subacute myocardial infarction (*11,12,14*). Segments with more reduced ^{123}I-BMIPP uptake than ^{99m}Tc-sestamibi uptake indicate jeopardized, but viable myocardium with a patent coronary artery (*14*). Matsunari et al. (*13*) reported that segments with reduced ^{123}I-BMIPP uptake show ^{201}Tl redistribution on exercise-redistribution ^{201}Tl imaging. It has been reported that myocardial area in which the uptake of ^{123}I-BMIPP is more decreased than that of perfusion tracer shows increased FDG uptake (*19*). These lines of evidence indicate that decreased ^{123}I-BMIPP uptake represents myocardial ischemia.

Iodine-123-BMIPP clearance is slow (approximately less than 10%), and thus ^{123}I-BMIPP is suitable for SPECT imaging. The precise mechanism of ^{123}I-BMIPP clearance from the ischemic myocardium remains still unknown. Iodine-123-BMIPP is trapped into the triglyceride (TG) fraction in the myocardium (*9,10*). It has been reported that the lipolysis of myocardial triglyceride is enhanced during low-flow ischemia and anoxia in the isolated rat heart (*29,30*). Since TG turnover is enhanced during myocardial ischemia, ^{123}I-BMIPP clearance may be increased. In the present study, ^{123}I-BMIPP clearances from ischemic and nonischemic myocardium were 9% ± 5% and 6% ± 8%, respectively, but this was not statistically significant. After oral glucose loading, clearance of ^{123}I-BMIPP was markedly increased in both ischemic and nonischemic myocardium, and ^{123}I-BMIPP clearance after glucose loading was faster in the ischemic area than in the nonischemic area (33% ± 8% versus 25% ± 9%, $p < 0.05$). Groot et al. (*31*) reported that lactate stimulates TG turnover in the ischemic myocardium through increased glycerol 3-phosphate levels. Since glucose increases glycerol 3-phosphate levels as lactate, it has been suggested that glucose loading enhanced TG turnover in the ischemic myocardium. This may explain the present results that ^{123}I-BMIPP clearance in the ischemic myocardium was faster than that in the nonischemic myocardium after glucose loading. Since clearance of ^{123}I-BMIPP was faster in the ischemic area, myocardial uptake of ^{123}I-BMIPP in the ischemic area was reduced after glucose loading.

Recently, myocardial FDG uptake can be visualized with a standard gamma camera (*32*). Since gamma camera systems are more readily available than PET, FDG-SPECT enables the application of FDG in routine clinical practice. However, special collimator and cyclotron are needed for FDG-SPECT because of the high-energy and short half-life of ^{18}F.

In the present study, two patients with normal coronary artery showed slight reduction of ^{123}I-BMIPP uptake in the inferior wall of the left ventricle, although ^{99m}Tc-sestamibi images of these patients were normal. One patient had left ventricular hypertrophy due to hypertension, and the presence of metabolic abnormality has been suggested. Since liver activity of ^{123}I-BMIPP was markedly increased in another patient, this high liver activity may hamper image interpretation of the left ventricular myocardium.

Since clearance of ^{123}I-BMIPP was faster in the ischemic area than in the nonischemic area after glucose loading, the decrease of ^{123}I-BMIPP uptake is more pronounced after glucose loading, and thus glucose loading enhanced the detection of ischemic myocardium by ^{123}I-BMIPP. In the present study, however, image quality was insufficient due to rapid ^{123}I-BMIPP clearance (38%) in one patient. This patient had coronary stenosis of exceeding 90% in the left anterior descending artery and right coronary artery and 75% stenosis in the left circumflex artery. The rapid ^{123}I-BMIPP clearance from the entire left ventricle may interfere with image interpretation in some patients with multivessel coronary disease.

In patients with angina pectoris, repeated episodes of transient ischemia may result in the impairment of myocardial fatty acid metabolism (*33*). We reported that decreased myocardial uptake of ^{123}I-BMIPP was frequently observed in the presence of normal myocardial ^{99m}Tc-sestamibi distribution, and metabolic imaging with ^{123}I-BMIPP was more sensitive for detecting myocardial ischemia than perfusion imaging with ^{99m}Tc-sestamibi in patients with stable and unstable angina (*17,18*). A noninvasive approach for the assessment of the presence and severity of ischemic myocardium is desirable, since a provocation test, either exercise or pharmacological stress, is usually contraindicated in unstable angina. However, the sensitivity and specificity of ^{123}I-BMIPP imaging for the detection of coronary artery disease were not good enough for a satisfactory diagnosis. In the present study, the sensitivity of resting ^{123}I-BMIPP imaging for the detection of coronary artery disease was 55% in

the fasting condition. After oral glucose loading, the sensitivity increased to 75% without a reduction of specificity (78%).

CONCLUSION

Oral glucose loading is a simple technique to enhance the detection of impaired myocardial fatty acid metabolism, and ^{123}I-BMIPP imaging with glucose loading may be a new approach for the noninvasive diagnosis of coronary artery disease.

ACKNOWLEDGMENTS

We thank Mr. Yoshifumi Shirakami (Nihon-Mediphysics) for the Discussion section. This study was supported in part by grants-in-aid for Scientific Research (grant no. 08770488) from the Ministry of Education, Science and Culture, Japan.

REFERENCES

1. Neely R, Rovetto J, Oram F. Myocardial utilization of carbohydrate and lipids. *Prog Cardiovasc Dis* 1972;15:289–299.
2. Lerch R, Ambos H, Bergmann S, Welch M, Ter-Pogossian M, Sobel B. Localization of viable, ischemic myocardium by PET with ^{11}C-palmitate. *Circulation* 1981;64: 689–699.
3. Shelbert H, Henze E, Schon H, et al. Carbon-11-palmitate for the noninvasive evaluation of regional myocardial fatty acid metabolism with positron computed tomography. III. In vivo demonstration of the effects of substrate availability on myocardial metabolism. *Am Heart J* 1983;105:492–504.
4. Van der Wall E, Heidendal G, Hollander W, Westera G, Roos J. Iodine-123-labeled hexadecanoic acid in comparison with ^{201}Tl for myocardial imaging in coronary heart disease. *Eur J Nucl Med* 1980;5:401–405.
5. Kennedy P, Corbett J, Kulkarni P, et al. Iodine-123-phenylpentadecanoic acid myocardial scintigraphy: usefulness in the identification of myocardial ischemia. *Circulation* 1986;74:1007–1015.
6. Kropp J, Likungu J, Kirchhoff P, et al. SPECT imaging of myocardial oxidative metabolism with 15-(p-(^{123}I) iodophenyl) pentadecanoic acid in patients with coronary artery disease and aorto-coronary bypass graft surgery. *Eur J Nucl Med* 1991;18:467–474.
7. Chouraqui P, Maddahi J, Henkin R, Karesh S, Galie E, Berman D. Comparison of myocardial imaging with iodine-123-iodophenyl-9-methyl pentadecanoic acid and thallium-201-chloride for assessment of patients with exercise-induced myocardial ischemia. *J Nucl Med* 1991;32:447–452.
8. Walamies M, Turjanmaa V, Koskinen M, Uusitalo A. Diagnostic value of ^{123}I-phenylpentadecanoic acid (IPPA) metabolic and thallium-201 perfusion imaging in stable coronary artery disease. *Eur Heart J* 1993;14:1079–1087.
9. Knapp F, Goodman M, Ambrose K, et al. The development of radioiodinated 3-methyl-branched fatty acids for evaluation of myocardial disease by single photon techniques. In: Van der Wall EE, ed. *Noninvasive imaging of cardiac metabolism.* Dordrecht: Martinus Nijhoff Publishers; 1987:159–201.
10. Knapp FF, Kropp J, Goodman M, et al. The development of iodine-123-methyl-branched fatty acids and their applications in nuclear cardiology. *Ann Nuklearmedizin* 1993;7:1–14.
11. Tamaki N, Kawamoto M, Yonekura Y, et al. Regional metabolic abnormality in relation to perfusion and wall motion in patients with myocardial infarction: assessment with emission tomography using an iodinated branched fatty acid analog. *J Nucl Med* 1992;33:659–667.
12. Geeter F, Franken P, Knapp F, Bossuyt A. Relationship between blood flow and fatty acid metabolism in subacute myocardial infarction: a study by means of ^{99m}Tc-sestamibi and ^{123}I-beta-methyl-iodo-phenyl pentadecanoic acid. *Eur J Nucl Med* 1994;21:283–291.
13. Matsunari I, Saga T, Taki J, et al. Kinetics of iodine-123-BMIPP in patients with prior myocardial infarction: assessment with dynamic rest and stress images compared with stress thallium-201 SPECT. *J Nucl Med* 1994;35:1279–1285.
14. Franken P, Geeter F, Dendale P, Demoor D, Block P, Bossuyt A. Abnormal free fatty acid uptake in subacute myocardial infarction after coronary thrombolysis: correlation with wall motion and inotropic reserve. *J Nucl Med* 1994;35:1758–1765.
15. Knapp F, Franken P, Kropp J. Cardiac SPECT with iodine-123-labeled fatty acids: evaluation of myocardial viability with BMIPP. *J Nucl Med* 1995;36:1022–1030.
16. Knapp F, Kropp J. Iodine-123-labeled fatty acids for myocardial single-photon emission tomography: current status and future perspectives. *Eur J Nucl Med* 1995;22:361–381.
17. Takeishi Y, Sukekawa H, Saito H, et al. Impaired myocardial fatty acid metabolism detected by ^{123}I-BMIPP in patients with unstable angina pectoris: comparison with perfusion imaging by ^{99m}Tc-sestamibi. *Ann Nuklearmedizin* 1995;9:125–130.
18. Takeishi Y, Sukekawa H, Saito H, et al. Clinical significance of decreased myocardial uptake of ^{123}I-BMIPP in patients with stable effort angina pectoris. *Nucl Med Commun* 1995;16:1002–1008.
19. Tamaki N, Kawamoto M, Yonekura Y, et al. Decreased uptake of I-123-BMIPP as a sign of enhanced glucose utilization assessed by FDG-PET [Abstract]. *J Nucl Med* 1991;32:1034.
20. Yamamichi Y, Kusuoka H, Morishita K, et al. Metabolism of iodine-123-BMIPP in perfused rat hearts. *J Nucl Med* 1995;36:1043–1050.
21. Ishii Y, MacIntyre WJ, Pritchard W, Eckstein R. Measurement of total myocardial blood flow in dogs with 43K and the scintilation camera. *Cir Res* 1973;33:113–122.
22. Yamakado K, Takeda K, Kitano T, et al. Serial changes of iodine-123-metaiodobenzylguanidine (MIBG) myocardial concentration in patients with cardiomyopathy. *Eur J Nucl Med* 1992;19:265–270.
23. Kurata C, Wakabayashi Y, Shouda S, et al. Enhanced cardiac clearance of iodine-123-MIBG in chronic renal failure. *J Nucl Med* 1995;36:2037–2043.
24. Takeishi Y, Chiba J, Abe S, Tonooka I, Komatani A, Tomoike H. Heterogeneous myocardial distribution of iodine-123 15-(p-iodophenyl)-3-R, S-methylpentadecanoic acid (BMIPP) in patients with hypertrophic cardiomyopathy. *Eur J Nucl Med* 1992;19:775–782.
25. Knuuti M, Nuutila P, Ruotsalainen U, et al. Euglycemic hyperinsulinemic clamp and oral glucose load in stimulating myocardial glucose utilization during PET. *J Nucl Med* 1992;33:1255–1262.
26. Schelbert H. Euglycemic hyperinsulinemic clamp and oral glucose load in stimulating myocardial glucose utilization during PET. *J Nucl Med* 1992;33:1263–1266.
27. Tamaki N, Yonekura Y, Konishi J. Myocardial FDG-PET studies with fasting, oral glucose loading or insulin clamp methods. *J Nucl Med* 1992;33:1263–1268.
28. Tamaki N, Yonekura Y, Yamashita K, et al. Positron emission tomography using fluorine-18-deoxyglucose in evaluation of coronary artery bypass grafting. *Am J Cardiol* 1989;64:860–865.
29. Schoonderwoerd K, Broekhoven-Schokker S, Hulsmann WC, Stam H. Enhanced lipolysis of myocardial triglycerides during low-flow ischemia and anoxia in the isolated rat heart. *Basic Res Cardiol* 1989;84:165–173.
30. Schoonderwoerd K, Broekhoven-Schokker S, Hulsmann WC, Stam H. Involvement of lysosome-like particles in the metabolism of endogeneous myocardial triglycerides during ischemia/reperfusion. Uptake and degradation of triglycerides by lysosomes isolated from rat heart. *Basic Res Cardiol* 1990;85:153–163.
31. Groot M, Willemsen P, Coumans W, Bilsen M, Vusse G. Lactate-induced stimulation of myocardial triacylglycerol turnover. *Biochim Biophys Acta* 1989;1006:111–115.
32. Huitink JM, Visser FC, Lingen A, et al. Feasibility of planar fluorine-18-FDG imaging after recent myocardial infarction to assess myocardial viability. *J Nucl Med* 1995;36: 975–981.
33. Vyska M, Machulla H, Stremmel W, et al. Regional myocardial free fatty acid extraction in normal and ischemic myocardium. *Circulation* 1988;78:1218–1233.